Exciton quantization and polariton propagation in semiconductor slabs: From semi-infinite crystals to quantum wells

A. D'Andrea
Istituto di Metodologie Avanzate Inorganiche del Consiglio Nazionale delle Ricerche, Area della Ricerca di Roma, Casella Postale 10, I-00016 Monterotondo Stazione, Roma, Italy

R. Del Sole
Dipartimento di Fisica, II Università degli Studi di Roma, "Tor Vergata," via O. Raimondo, I-00173 Roma, Italy
(Received 24 April 1989; revised manuscript received 18 August 1989)

Variational wave functions are proposed for the two lowest states of excitons in thin slabs. They are shown to be reliable for CdS slabs of thickness L larger than 2.5 exciton radii a_B. The energy difference between them is close to that found by quantizing the center-of-mass motion in a slab of effective thickness L-2d, where d is the transition-layer depth. This approximate rule becomes exact for $L > 16a_B$. The calculated optical properties show that absorptance maxima and transmittance minima are in close correspondence with CdS exciton levels for $L < 500$ Å, where polaritonic effects are not important.

I. INTRODUCTION

It is well known that the wave functions of Wannier excitons are very sensitive to the different kinds of confinement. Even a semi-infinite crystal, namely the weakest confinement, affects wave functions and other exciton properties in a nontrivial way, as can be inferred from the enormous amount of literature dealing with the dead layer and additional boundary conditions.[1-8]

Reliable exciton wave functions are available only for slabs much thicker than the exciton radius ($L \gg a_B$) or in the quantum-well (QW) limit ($L < a_B$). In the former case, Cho and Kawata (CK) (Ref. 9) have extended the approach of D'Andrea and Del Sole (DA-DS) (Refs. 5-8), valid for semi-infinite crystals, to slabs. DA-DS describe the distortion of the exciton wave function near the surface (at $z=0$) using an evanescent wave of the form $\exp(-Pz)$ for the translational motion, which partially cancels the contributions of the incoming and reflected waves in a transition layer of depth $1/P$ near the surface. Such a transition layer is similar to the dead layer proposed by Thomas and Hopfield[2] on the basis of an intuitive model. In the method of CK, the DA-DS wave function appropriate to the front surface is matched in the middle of the slab to that of the back surface. In this case the P value is the same as for semi-infinite crystals, while the center-of-mass motion is quantized as an effect of the confinement of the slab. The validity of the method relies on the assumption that the two transition layers associated with the two surfaces do not interact, namely that $\exp(-PL) \ll 1$.

In this paper we want to overcome such a limitation by extending this approach to thinner slabs. In this case terms proportional to $\exp(-PL)$, which have been neglected by CK,[9] must be retained. Moreover, the P value for thin slabs is likely different from that used in semi-infinite crystals. In order to clarify this point, we fix some value of P and calculate the wave functions as CK do, but retain the exponential terms. Then we consider such wave functions as variational wave functions, and compute the mean value of the exciton Hamiltonian on them. Finally the minimum of such value is found by varying P and the effective Bohr radius a for the two lowest quantized states. The optical spectrum is computed without introducing further approximations by using a method very similar to the additional-boundary-condition (ABC) -free approach of Cho.[10] A further advantage of this method is that it is appropriate for very thick as well as very thin slabs.

Our purpose is to reach the QW limit, namely the range $L \leq a_B$, in order to fill the existing gap between exciton wave functions in thick slabs and in QW's. In QW's, a series of exciton states is associated with each pair of electron and hole subbands. The lowest exciton state of our method corresponds to the QW exciton ground state, arising from the lowest conduction and the highest valence subband. The validity of our variational approach is limited by the capability of bulk-derived wave functions to be distorted in the QW geometry. Such a capability has been checked by comparison, in the case of CdS, with the variational QW wave functions of Bastard *et al.*[11] and of Shinouza and Matsuura.[12] The agreement is good for $L > 2.5a_B$, where our approach yields a slightly lower-energy exciton. For $L < 2.5a_B$, the energy resulting from our calculation rises steeply, since the bulk-derived wave function cannot sustain the large distortion due to the QW confinement. In the latter range therefore the present approach is not valid; nevertheless, it closes the gap present until now for intermediate slab thicknesses. We find that the exciton quantization in the intermediate-thickness range is determined by the center-of-mass motion, and not, as recently hypothesized,[13] by the electron and hole *separate* quantization. We also find that the second quantized exciton level

is particularly sensitive to the value of the transition-layer depth $1/P$, so that it might be used as a tool to determine P from optical experiments.

In Sec. II we describe slab wave functions. The calculation of the optical properties is outlined in Sec. III, while the results are discussed in Sec. IV. The main findings of the present work are summarized in Sec. V.

II. WANNIER-EXCITON WAVE FUNCTIONS IN SLABS

The aim of this section is to derive realistic wave functions for excitons in slabs of any thickness L, namely from quantum wells to semi-infinite solids.

In the quantum-well limit ($L \leq a_B$), an appropriate variational wave function for the lowest exciton level associated with the nth electron and hole subband of a slab $-L/2 < z < L/2$, is[11]

$$\Psi(z_e,z_h,\rho)=N_0\cos(K_n z_e)\cos(K_n z_h)\exp(-r/a)\ , \tag{1}$$

where N_0 is the normalization constant, a is a variational parameter, $r=|r_e-r_h|=[\rho^2+(z_e-z_h)^2]^{1/2}$, and the electron and the hole are quantized separately along the z axis. Imposing the boundary conditions at surfaces ($z=\pm L/2$), we find $K_n=n\pi/L$. This wave function has the correct behavior in the two-dimensional–exciton limit ($L\to 0$), as shown in Ref. 11. The lowest exciton states of different symmetries may be obtained by multiplying the variational wave function (1) by r-dependent functions of the appropriate symmetry.[12]

On the other hand, for semi-infinite crystals ($z>0$), an appropriate wave function is[5]

$$\Psi(z,Z,\rho)=(\exp(-iKZ)+A\exp(iKZ)-\{\exp[-iKs(z)|z|]+A\exp[iKs(z)|z|]\}\exp(-PZ))\exp(-r/a)/(2\pi)^{1/2}\ , \tag{2}$$

where $z=z_e-z_h$, $s(z)=m_h/M$ for $z>0$, and $s(z)=m_e/M$ for $z<0$,

$$Z=\frac{m_e}{M}z_e+\frac{m_h}{M}z_h \text{ and } A=-\frac{P-iK}{P+iK}\ .$$

The first two terms in the boldface parentheses in Eq. (2) are the incident and reflected excitons at the surface, while the other terms, multiplying the evanescent wave $\exp(-PZ)$, mimic the virtually excited Rydberg states of the exciton with principal quantum numbers $n>1$. These terms come from the fulfillment of the no-escape boundary conditions:

$$\Psi(z_e=0)=\Psi_h(z_h=0)=0\ . \tag{3}$$

Recently the authors have computed the exciton reflectivity of CdS using a microscopic theory based on the exciton wave function (2), obtaining a quantitative accord with experimental results;[7] moreover, a fair accord was obtained for many different semiconductors.[14]

This approach has been later extended by Cho and Kawata to thick slabs.[9] The validity of such work relies on the assumption of noninteracting transitions layers, namely $\exp(-PL)\ll 1$.

In the intermediate range of slab dimensions, between quantum wells and thick slabs, reliable wave functions for Wannier excitons are not available in the literature. For closing this gap we cope with the case of thin slabs, by taking into account the terms of the order $\exp(-PL)$, neglected by CK. Since the exciton Hamiltonian is invariant under reflection through the central plane of the slab ($z=0$), namely for $(z_e,z_h)\to(-z_e,-z_h)$, we can consider separately wave functions of even and odd parity. Let us consider the most general even wave functions of energy $E=\varepsilon_{1s}+\hbar^2K^2/2M$, obtained extending the approach of Refs. 6 and 8 to slabs:

$$\Psi^e_K(r,Z)=N^e[\cos(KZ)\phi_{1s}(r)+\sum_{(n\ \text{even})}c_n\cosh(P_nZ)\phi_n(r)+\sum_{(n\ \text{odd})}c_n\sinh(P_nZ)\phi_n(r)]\ , \tag{4}$$

where $\phi_{1s}(r)$ is the hydrogenic state, $\phi_n(r)$ are the excited states of energy ε_n, and $P_n=[2M(\varepsilon_n-E)/\hbar^2]^{1/2}$. The sum over n even (n odd) means that only hydrogenic functions which are even (odd) with respect to $z\to -z$ must be considered. If we limit the exciton energy to $E<\varepsilon_2$, in the spirit of Ref. 5, we can approximate the P_n's by some mean value P, obtaining for the even wave functions

$$\Psi^e_K(r,Z)=N^e[\cos(KZ)-F_{ee}(z)\cosh(PZ)+F_{eo}(z)\sinh(PZ)]\exp(-r/a)\ , \tag{5}$$

where N^e is the normalization constant, the functions $F_{ee}(z),F_{eo}(z)$ are general even and odd functions of z, respectively, and the explicit form of ϕ_{1s} has been used. The fulfillment of the no-escape boundary conditions (3) yields, for $z>0$,

$$F_{ee}(z)=[\sinh(PZ_1)\cos(KZ_2)-\sinh(PZ_2)\cos(KZ_1)]/\sinh[P(Z_1-Z_2)]\ , \tag{6}$$

$$F_{eo}(z)=[\cosh(PZ_1)\cos(KZ_2)-\cosh(PZ_2)\cos(KZ_1)]/\sinh[P(Z_1-Z_2)]\ , \tag{7}$$

where $Z_1=L/2-m_hz/M$, $Z_2=-L/2+m_ez/M$. Even

though $F_{ee}(z)$ and $F_{eo}(z)$ have discontinuous derivatives at $Z=0$, the total wave function must have a continuous derivative. This requirement leads to the quantization of the center-of-mass momentum K:

$$K_n \tan(K_n L/2)+P\tanh(PL/2)=0 , \tag{8}$$

for $n=1,3,5,\ldots$. [In order of increasing K_n, the $n=2,4,6,\ldots$ values will belong to odd wave functions, as can be easily seen from the quantization conditions (8) and (12).]

Analogously, for the odd wave functions,

$$\Psi^o_K(z,Z,\rho)=N^o[\sin(KZ)+F_{oe}(z)\sinh(PZ) -F_{oo}(z)\cosh(PZ)]\exp(-r/a) , \tag{9}$$

where N^o are the normalization constants, and the functions $F_{oe}(z), F_{oo}(z)$ are

$$F_{oe}(z)=[\cosh(PZ_1)\sin(KZ_2) -\cosh(PZ_2)\sin(KZ_1)]/\sinh[P(Z_1-Z_2)] , \tag{10}$$

$$F_{oo}(z)=[\sinh(PZ_1)\sin(KZ_2) -\sinh(PZ_2)\sin(KZ_1)]/\sinh(P(Z_1-Z_2)] . \tag{11}$$

The quantized center-of-mass momentum K is given by the equation

$$\frac{\tan(K_n L/2)}{K_n}-\frac{\tanh(PL/2)}{P}=0 , \tag{12}$$

for $n=2,4,6,\ldots$. Obviously, in the limit $L\to\infty$ the slab wave functions (5) and (9) recover the correct wave function (2) appropriate to a semi-infinite sample.

Cho and Kawata[9] have already treated the particular case of thick slabs, where the interaction of the two surfaces, proportional to $\exp(-PL)$, can be neglected. When the interaction between the two transition layers is considered, the values of the parameters P and a may be different from the values appropriate to semi-infinite crystals. Therefore they are considered here as variational parameters to be adjusted in order to minimize the $n=1,2$ exciton energies. In the Appendix we give all formulas necessary for performing the variational calculations. It should be noticed that, since variational wave function (5) is different from (4), its energy will be different from $\varepsilon_{1s}+\hbar^2K_n^2/2M$. The same is obviously true for the odd wave functions (9). As a consequence, the restriction $E<\varepsilon_2$ can be relieved.

The values of a and P as functions of L are shown in Figs. 1 and 2 for CdS. In the calculation we have used the parameter values $\varepsilon_0=8.1$, $M=0.94m$, $\mu=0.135m$, and $\mathcal{R}^*=28$ meV. In Fig. 1 it is also shown the value of the a parameter obtained using the QW trial wave function (1).[11] While the parameter a for even ($n=1$) and odd ($n=2$) wave functions reaches its bulk value $a_B=32$ Å already for $L=4a_B$ (see Fig. 1), the transition layer depth $d=1/P$ shows a slower convergence and different curves for even $n=1$ and odd $n=2$ wave functions (see Fig. 2). As $L\to\infty$, P saturates to $P_\infty=0.02$ Å^{-1}, which is smaller than the bulk value $P=0.45$ Å^{-1}.[8] This discrepancy is probably due to the variational framework used in the present approach.

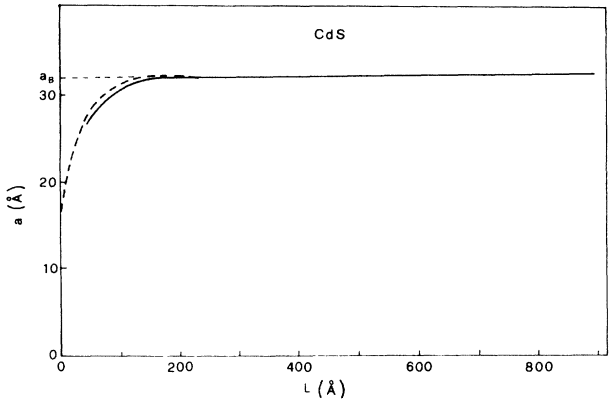

FIG. 1. The variational parameter a of the exciton ground state shown as a function of the slab thickness L. The exciton parameters are: $\varepsilon_0=8.1$, $M=0.94$, $\mu=0.135m$. Dashed line: Bastard *et al.* (Ref. 11). Solid line: present calculation.

The minimized energy for the $n=1$ and $n=2$ excitons is shown in Fig. 3. The validity of the even wave function in the quantum-well limit is checked by comparing its variational energy with that obtained minimizing the energy according to Eq. (1), as shown in the inset of Fig. 3. The energy of the $n=2$ state is always lower, for $L>100$ Å, than that of the second QW level, namely the $2p_x$-like level of Ref. 12. In conclusion, the present approach is reliable for $L>2.5a_B$. In this range, it yields exciton energies slightly lower than the corresponding energies computed using the QW wave functions, which do not account properly of the center-of-mass kinetic energy.

It was speculated[13] that the exciton levels follow the

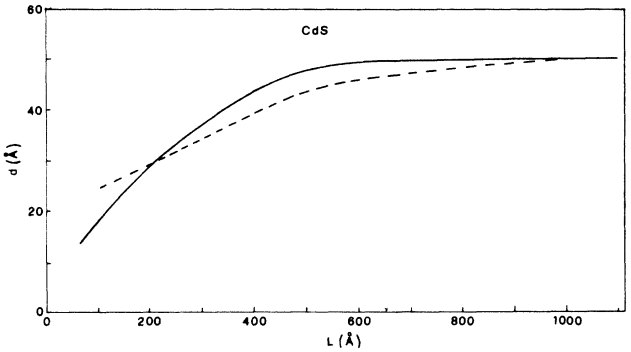

FIG. 2. The variational parameter $d=1/P$ (transition-layer depth) shown as a function of the slab thickness L. Solid line: lowest exciton state of even parity for reflection with respect to the central plane of the slab. Dashed line: lowest exciton state of odd parity. Exciton parameters as in Fig. 1.

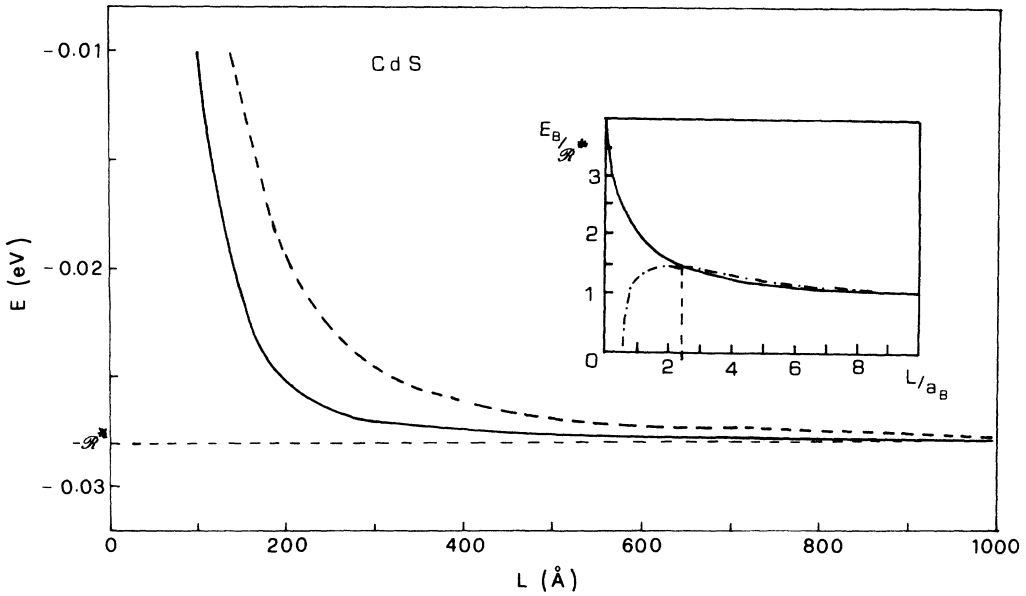

FIG. 3. The exciton energy E, measured from the bottom of the infinite-crystal conduction band, as a function of the slab thickness L. Solid line: lowest exciton state of even parity ($n=1$). Dashed line: lowest exciton state of odd parity ($n=2$). The binding energy in the slab $E_B=\hbar^2\pi^2/(2\mu)-E$ of the lowest even exciton is shown in the inset in units of the bulk effective Rydberg $\mathcal{R}^*$. Solid line: Bastard *et al.* (Ref. 11). Dotted-dashed line: present calculation. Exciton parameters as in Fig. 1.

separate electron and hole quantization

$$E_n=\frac{\hbar^2 n^2\pi^2}{2\mu L^2}+\text{const}\ , \tag{13}$$

not only in QW's, but even in GaAs slabs as thick as $10a_B$. However, this assumption strongly contrasts with our results for CdS, where for $L=200$ Å$=6a_B$ we find $E_2-E_1=5$ meV, while (13) yields $E_2-E_1=21$ meV. In our calculation, the energy difference E_2-E_1 is much closer to the result obtained by quantizing the center-of-mass motion in a slab of thickness $L-2/P$:

$$E_n=-\mathcal{R}^*+\frac{n^2\hbar^2\pi^2}{2M(L-2/P)^2}\ , \tag{14}$$

where P is the average between P_1 and P_2. This equation is correct for $L\gg 1/P$, since in this case $P_1=P_2$ (see Fig. 2), $K_n=n\pi/(L-2/P)$,[9] and $E_n=-\mathcal{R}^*+\hbar^2K_n^2/2M$. Actually the deviation of the exciton energy from the latter equation is due to the evanescent wave in (2), coupling the relative and center-of-mass motions. As $L\to\infty$, its contribution to the energy vanishes as $O(1/PL)$. Nevertheless, Eq. (14) qualitatively accounts for E_2-E_1 also for slabs as small as $L=200$ Å in CdS: it yields 6 meV, which compares well with the variational value of 5 meV. The difference becomes smaller than 0.02 meV for $L>500$ Å. In this range ($L>16a_B$) we can use Eq. (14) for the exciton energy, as CK do, while the interaction between the two transition layers still affects the value of P, which is 10% lower than P_∞. In view of the simple relation between exciton energy, slab thickness, and transition-layer depth, energy measurements in this energy range are appropriate to determine the P value.

In Fig. 4 we show the quantity $|\Psi(\mathbf{r}=0,Z)|^2$, relevant for the optical response, computed for quantum-well wave function (1) and for the even wave function $n=1$ (5), in the case of a slab of $L=100$ Å. The two curves are very similar, indicating that both wave functions, at this L value, are good approximations of the true exciton

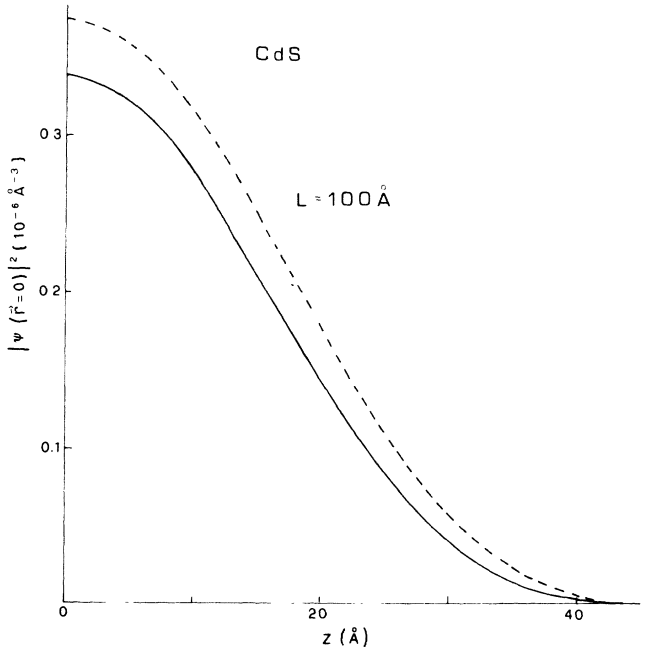

FIG. 4. $|\Psi(0,Z)|^2$ of excitons in a 100-Å-thick CdS slab. Solid line: lowest even exciton computed according to the present formulation. Dashed line: lowest even exciton computed according to Ref. 11. Exciton parameters as in Fig. 1.

wave function.

In conclusion, we can distinguish in CdS three different ranges of thicknesses with respect to Wannier exciton wave functions, namely, (a) the quantum-well zone, from $L=0$ to $L=2.5a_B$, where the electron and the hole are quantized separately along the z axis and a reliable ground-state wave function is given in Eq. (1); (b) for $2.5a_B<L<16a_B$, where our approach is valid and the exciton quantization approximately follows the center-of-mass rule (14); and (c) from $L=16a_B$ to semi-infinite samples, where the exciton energy is well described by $\varepsilon_{1s}+\hbar^2K_n^2/2M$ and the center-of-mass rule (14) is correct. In the last range the CK approach is valid.[9]

III. NORMAL-INCIDENCE OPTICAL RESPONSE OF A SLAB

For computing the normal-incidence optical response of a slab, we must consider three different zones of the space. In the first zone, $-\infty<z<-L/2$, the total electric field is

$$\mathcal{E}(z)=\exp[i\omega(z+L/2)/c] +r\exp[-i\omega(z+L/2)/c] , \tag{15}$$

where r is the reflection amplitude, and c is the light velocity in vacuum. In the zone $L/2<z<\infty$, the transmitted electric field is

$$\mathcal{E}(Z)=t\exp[i\omega(z-L/2)/c] , \tag{16}$$

where t is the transmission amplitude; finally, in the slab, $-L/2<z<L/2$, the electric field is

$$\mathcal{E}(Z)=A\exp(iqZ)+B\exp(-iqZ)+\mathcal{E}_p , \tag{17}$$

where $q=\omega[\varepsilon_0/C]^{1/2}$ and $\mathcal{E}_p$ is a particular solution of Maxwell's integro-differential equation:

$$\frac{d^2\mathcal{E}}{dz^2}+\frac{\omega^2}{c^2}\varepsilon_0\mathcal{E}+\frac{\omega^2}{c^2}\sum_k A_k\Psi_k(z) \times\int_{-L/2}^{L/2}\Psi_k(z')\mathcal{E}(z')dz'=0 . \tag{18}$$

Here

$$A_K=\frac{S}{K^2-q_0^2} ,$$

$$q_0^2=2M(\hbar\omega-\hbar\omega_{\mathrm{TO}}-\hbar^2K_{\parallel}^2/2M+i\Gamma)/\hbar^2 ,$$

and $S=(16\pi e^2M)/(m\omega^2\hbar^2)|p_{vc}|^2$, where p_{vc} is the matrix element of the dipole moment between valence and conduction bands, and Γ is the lifetime broadening. The third term in (18) embodies the exciton dielectric susceptibility computed from the wave functions $\Psi_K(z)$ discussed in Sec. II. Only a finite number of quantized states Ψ_K can be retained in (18); we will discuss in Sec. IV how to choose such number. If we define the following quantity:

$$F(z)=-\frac{\omega^2}{c^2}\sum_K A_K\Psi_K(z)I_K , \tag{19}$$

where

$$I_K=\int_{-L/2}^{L/2}\Psi_K(z')\mathcal{E}(z')dz' , \tag{20}$$

the propagation equation (18) becomes:

$$\frac{d^2}{dz^2}\mathcal{E}(z)+\frac{\omega^2}{c^2}\varepsilon_0\mathcal{E}(z)+F(z)=0 , \tag{21}$$

which admits as a particular solution:

$$\mathcal{E}_p(z)=-\frac{1}{2iq}\int_0^z\{\exp[iq(z-z')] -\exp[-iq(z-z')]\}F(z')dz' . \tag{22}$$

The electric field in the slab therefore becomes

$$\mathcal{E}(z)=A\exp(iqz)+B\exp(-iqz) -\frac{1}{2iq}\int_0^z dz'\{\exp[iq(z-z')] -\exp[-iq(z-z')]\}F(z') . \tag{23}$$

Now by inserting the electric field of the slab (23) into (18), we obtain a system of equations for the quantities I_K:

$$\sum_{K'}\left[\delta_{KK'}+\frac{\omega^2}{2iqc^2}C_{KK'}A_{K'}\right]I_{K'}=A\phi_K(-q)+B\phi_K(q) , \tag{24}$$

where

$$\phi_K(q)=\int_{-L/2}^{L/2}\Psi_K(z)\exp(-iqz)dz , \tag{25}$$

and

$$C_{KK'}=\int_{-L/2}^{L/2}dz\,\Psi_K(z)\int_0^z dz'\{\exp[iq(z-z')] -\exp[-iq(z-z')]\} \times\Psi_{K'}(z') . \tag{26}$$

We can solve the linear system (24) in terms of the matrix

$$M_{KK'}=\left[\delta_{KK'}+\frac{\omega^2}{2iqc^2}C_{KK'}A_{K'}\right]^{-1} . \tag{27}$$

The size of the matrix to be inverted is determined by the number of exciton states considered in (18).

The electric field and its first derivative inside the slab on the front (F) surface $Z=-L/2$ and on the back (B) surface $Z=L/2$ are, respectively,

$$\mathcal{E}_F=\alpha A+\beta B , \tag{28a}$$

$$\frac{d}{dZ}\mathcal{E}_F=\alpha' A+\beta' B , \tag{28b}$$

$$\mathcal{E}_B=\gamma A+\delta B , \tag{29a}$$

$$\frac{d}{dZ}E_B=\gamma' A+\delta' B , \tag{29b}$$

where

$$\alpha=\exp(-iqL/2)-\frac{\omega^2}{2iqc^2}\sum_K A_K[\exp(-iqL/2)\chi_K^F(-q)-\exp(iqL/2)\chi_K^F(q)]\sum_{K'} M_{KK'}\phi_{K'}(-q)\ , \tag{30}$$

$$\beta=\exp(iqL/2)-\frac{\omega^2}{2iqc^2}\sum_K A_K[\exp(-iqL/2)\chi_K^F(-q)-\exp(iqL/2)\chi_K^F(q)]\sum_{K'} M_{KK'}\phi_{K'}(q)\ , \tag{31}$$

$$\gamma=\exp(iqL/2)-\frac{\omega^2}{2iqc^2}\sum_K A_K[\exp(iqL/2)\chi_K^B(-q)-\exp(-iqL/2)\chi_K^B(-q)]\sum_{K'} M_{KK'}\phi_{K'}(-q)\ , \tag{32}$$

$$\delta=\exp(-iqL/2)-\frac{\omega^2}{2iqc^2}\sum_K A_K[\exp(iqL/2)\chi_K^B(-q)-\exp(-iqL/2)\chi_K^B(q)]\sum_{K'} M_{KK'}\phi_{K'}(q)\ , \tag{33}$$

and,

$$\alpha'=iq\exp(-iqL/2)-\frac{\omega^2}{2c^2}\sum_K A_K[\exp(-iqL/2)\chi_K^F(-q)+\exp(iqL/2)\chi_K^F(q)]\sum_{K'} M_{KK'}\phi_{K'}(-q)\ , \tag{34}$$

$$\beta'=-iq\exp(iqL/2)-\frac{\omega^2}{2c^2}\sum_K A_K[\exp(-iqL/2)\chi_K^F(-q)+\exp(iqL/2)\chi_K^F(q)]\sum_{K'} M_{KK'}\phi_{K'}(q)\ , \tag{35}$$

$$\gamma'=iq\exp(iqL/2)-\frac{\omega^2}{2c^2}\sum_K A_K[\exp(iqL/2)\chi_K^B(-q)+\exp(-iqL/2)\chi_K^B(q)]\sum_{K'} M_{KK'}\phi_{K'}(-q)\ , \tag{36}$$

$$\delta'=-iq\exp(-iqL/2)-\frac{\omega^2}{2c^2}\sum_K A_K[\exp(iqL/2)\chi_K^B(-q)+\exp(-iqL/2)\chi_K^B(q)]\sum_{K'} M_{KK'}\phi_{K'}(q)\ . \tag{37}$$

We have used the notations

$$\chi_K^F(q)=\int_0^{-L/2}\exp(iqz')\Psi_K(z')dz'\ , \tag{38}$$

$$\chi_K^B(q)=\int_0^{L/2}\exp(iqz')\Psi_K(z')dz'\ . \tag{39}$$

By matching the electric field at the interfaces in terms of the front (Z_F) and back (Z_B) impedences, we get the relations

$$Z_F=i\frac{\omega}{c}\frac{1-r}{1+r}=\frac{\alpha' A/B+\beta'}{\alpha A/B+\beta}\ , \tag{40}$$

$$Z_B=i\frac{\omega}{c}=\frac{\gamma' A/B+\delta'}{\gamma A/B+\delta}\ . \tag{41}$$

From (41) we get

$$A/B=-\frac{\delta'-i\omega\delta/c}{\gamma'-i\omega\gamma/c}\ . \tag{42}$$

Finally, the reflected and transmitted amplitudes are, respectively,

$$r=\frac{i\omega/c-Z_F}{i\omega/c+Z_F}\ , \tag{43}$$

$$t=\frac{\delta'+\delta+(\gamma'+\gamma)A/B}{\beta'+\beta+(\alpha'+\alpha)A/B}\left[1+r\frac{1-\omega/c}{1+\omega/c}\right]\ , \tag{44}$$

and the normalized absorptance is

$$A=(1-|r|^2-t|^2)/(1-|r|^2)\ . \tag{45}$$

In the next section we will discuss the optical properties of a slab of CdS as a function of its thickness.

IV. RESULTS

In this section we discuss the calculated optical properties, namely reflectance, transmittance, and absorptance, of excitons in thin CdS films. First we want to show how the results depend on the number of quantized exciton states retained in the expression of the slab susceptibility entering the propagation equation (18). Since their energy separation decreases as L increases, more and more states must be considered as L tends to infinity. In order to test the convergence for a quite large value of L, when many states must be retained, we show in Fig. 5 the computed reflectance of a self-sustained CdS slab of $L=500$ Å. The first four quantized states occur in the 5-meV range of energy shown in the figure. Inclusion of the fifth state in the calculation yields well converged results, differing very little from those obtained using $n=10$ or more. A similar test of convergence has been performed for all calculations of optical properties reported below.

The computed absorptance of a self-sustained CdS slab of thickness $L=300$ Å is shown in Fig. 6. The solid line is obtained starting from the exciton $n=1$ and $n=2$ levels both computed by energy minimization, as described in Sec. II. In particular, two different P values are used for these two levels. Absorption peaks correspond well to exciton levels, indicated by arrows, showing that polaritonic effects do not affect peak positions for this (and smaller) values of L. The reason is that only large k_n values are allowed by exciton quantization in thin films, for which the lower polariton dispersion curve is very close to the bare exciton dispersion, while the upper polariton, mostly photonlike, has too high energy to be excited by the incident radiation.[15]

A less-approximate approach was used in Ref. 16,

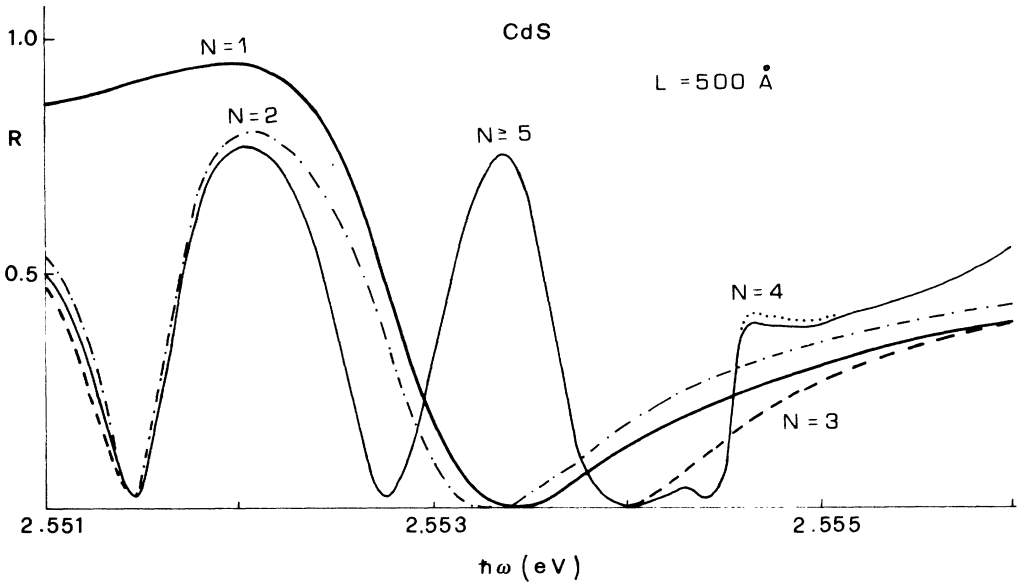

FIG. 5. Normal-incidence reflectance of a CdS slab of 500 Å. The calculations have been carried out retaining N exciton quantized states in the dielectric susceptibility. Exciton parameters as in Fig. 1, and $4\pi\alpha$ (oscillator strength)=0.013.

where only the $n=1$ energy was minimized, while the levels with $n>1$ were calculated according to the formula valid for thick slabs:

$$E_n = -\mathcal{R}^* + \hbar^2 K_n^2/(2M)\ , \tag{46}$$

with K_n given by (8) or (12). The absorptance calculated according to this approach is shown by the dotted-dashed line in Fig. 6. In order to compare our results with those of Cho and Ishihara (CI),[17] who have derived the optical properties exactly starting from the wave functions of CK,[9] we have computed all (including $n=1$) exciton levels from (8) and (12), using for P the P_∞-value, without any energy-minimization procedure. The only difference with respect to CI's approach is the inclusion of the very small terms of order $\exp(-PL)$. The results obtained in

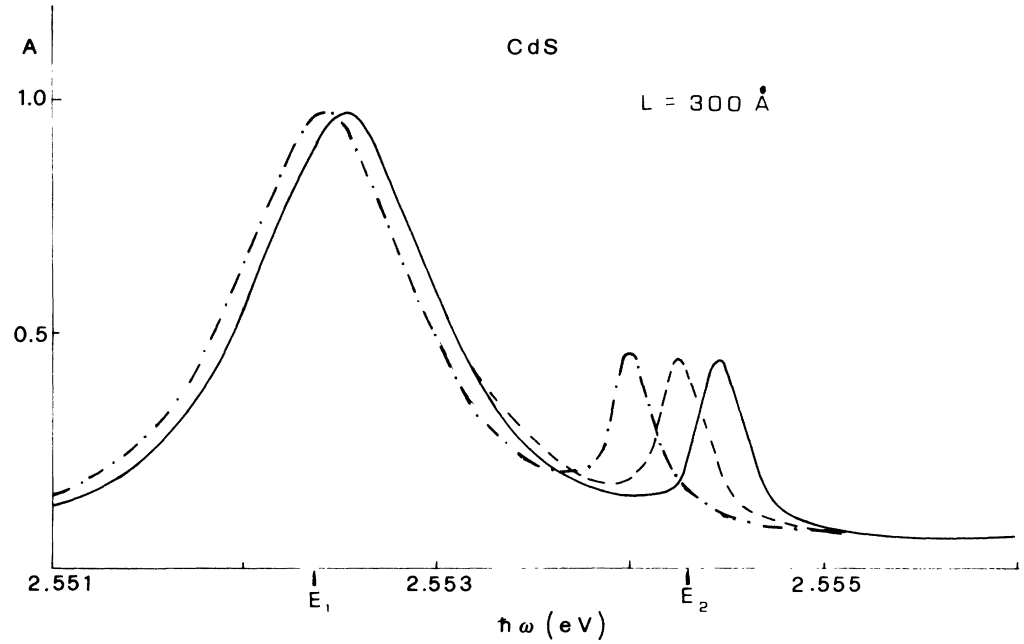

FIG. 6. Exciton normalized absorptance in a CdS slab of 300 Å. Solid line: exciton levels E_1 and E_2 (indicated by arrows) calculated by energy minimization. Dotted-dashed line: E_1 calculated by energy minimization and E_2 according to (46). Dashed line: E_1 and E_2 both calculated according to (46). Exciton parameters as in Fig. 5.

this framework are shown by the dashed line in Fig. 6. It is apparent that the energy of the $n=1$ level is poorly dependent on the type of approach (for $L=300$ Å), while larger differences occur for the second level. We notice that the partial minimization approach of Ref. 16 yields the $n=2$ level 0.5 meV lower than that given by the full minimization. This difference is mostly due to the fact that the energy expectation value is different from (46); only a minor amount comes from the different P_2 values (0.027 and 0.029 Å^{-1}) used in the two calculations. On the other hand, the difference between the CI-like curve (dashed line) and the partial minimization curve (dotted-dashed line) is only due to the different P values used (0.027 and 0.020 Å^{-1}).

As $L \to \infty$, P tends to P_∞, and the interaction between the two transition layers, responsible for the difference between the energy expectation value and (46), vanishes. In this case the three approaches yield the same result. This starts to be true for $L \geq 500$ Å $=16a_B$, where E_2-E_1 computed according to the CI approach is different from the full minimization approach by only 0.05 meV. In the range $16a_B \lesssim L \lesssim \lambda/2$ (if such a range exists), good conditions for the determination of P from absorptance measurements occur: the absorptance maxima are in close correspondence with the energy levels, and, moreover, the simple relation (14) between energy and P holds.

Finally it should be noticed the large width (1 meV) of the $n=1$ absorptance peak with respect to the broadening used in the calculation, that was only $\Gamma=0.1$ meV. This comes from the fact that the local (i.e., integrated over z) dielectric susceptibility, proportional to A_{K_1} [see Eq. (18)], is negative in some frequency range above E_1. As it occurs between ω_0 and ω_L in the bulk, the light wave vector is there imaginary, so that light is strongly absorbed.[18] As L becomes smaller and smaller, this effect becomes less important and the absorptance line shape becomes proportional to the imaginary part of the dielectric susceptibility[10] (namely of width Γ) for $L \ll (c\omega_{LT}/4\pi\alpha\omega_0^2)=200$ Å. We cannot reach this range in CdS, since we restrict ourselves to $L \geq 100$ Å, where our model is reliable.

The reflectance of the same CdS slab is shown in Fig. 7. It is apparent that the features related to the level $n=2$ are quite weak; therefore, though they show a similar dependence on E_2 as the corresponding absorptance features, a straightforward determination of P from them is more difficult.

The absorptance and transmittance of a CdS slab of $L=500$ Å are shown in Fig. 8. A first point to be noticed is that transmittance minima are in close correspondence with absorptance maxima (this is also true for smaller L values). In this case the absorptance maxima do not correspond to exciton levels, indicated by arrows. This is due to the coupling of excitons to photons, i.e., to polaritonic effects, which become more important as L increases.

In conclusion, for the optical properties of excitons in CdS slabs, we can distinguish two regimes. In the first one, for $L < 16a_B$, absorptance maxima and transmission minima are in close correspondence with quantized exciton levels, which must be computed using the full energy-minimization approach described in Sec. II. In the second regime, for $L \geq 16a_B$, the exciton levels are simply given by (14), but there is no straightforward correspondence between them and the features in the optical spectra. Therefore, we can conclude that the range where it is easy to check the present theory by optical experiments in CdS is for $2.5a_B < L < 16a_B$, where polaritonic effects can be neglected.

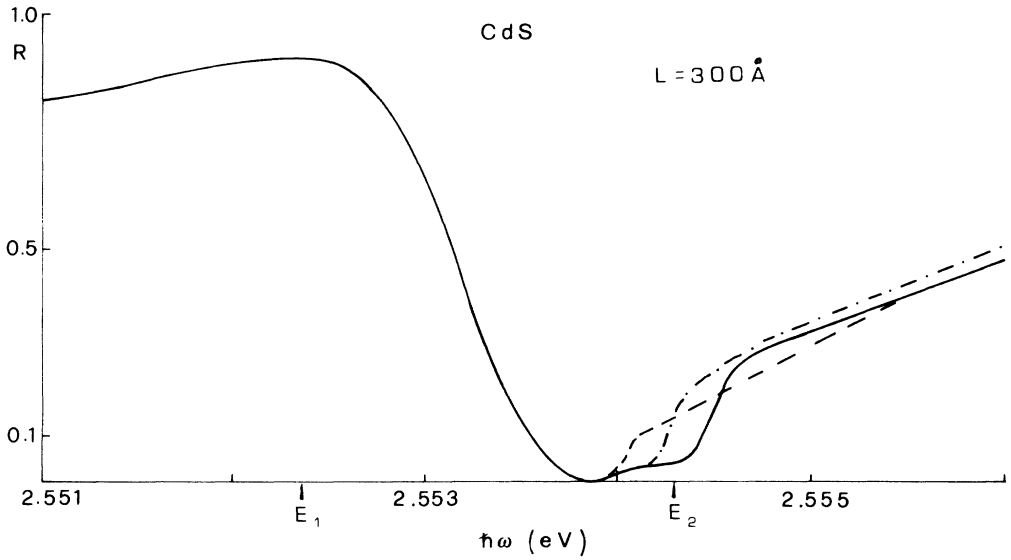

FIG. 7. Normal-incidence reflectance of a CdS slab of 300 Å. Solid line: exciton levels E_1 and E_2 (indicated by arrows) calculated by energy minimization. Dashed line: E_1 calculated by energy minimization and E_2 according to (46). Dotted-dashed line: E_1 and E_2 both computed according to (46). Exciton parameters as in Fig. 5.

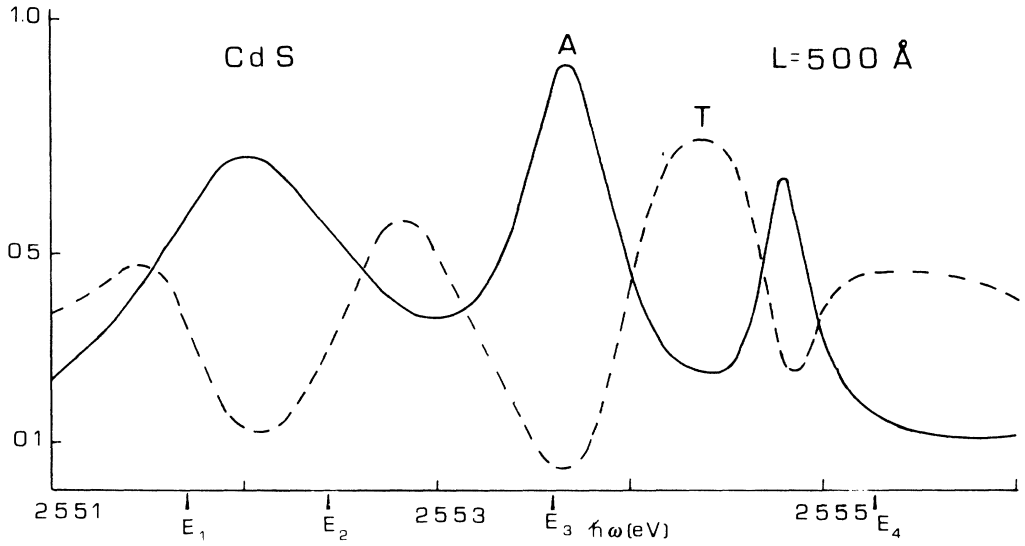

FIG. 8. Normalized absorptance A and transmittance T of a CdS slab of 500 Å. Exciton levels are indicated by arrows. E_1 and E_2 are computed by energy minimization and the higher levels according to (46). Exciton parameters as in Fig. 5.

V. CONCLUSIONS

The exciton wave function derived in this paper is valid for slabs thicker than $2.5a_B$. Therefore reliable wave functions are now available for all L values: our approach is complementary to that of Bastard *et al.*,[11] valid in the quantum-well regime, and embodies that of CK,[9] valid for $L > 16a_B$.

A difference in principle between the present approach and that developed by us in Refs. 6–8 for semi-infinite crystals should be emphasized. In Refs. 6–8 the analytical wave function depending on P is meant as an interpolation form, valid only for $\mathbf{r}=0$, and P is determined by comparison with the numerically exact wave function computed for $\mathbf{r}=0$. The same philosophy can be thought to underly the approach of Cho and co-workers,[9,17] which is valid when the surfaces do not interact. On the other hand, the present approach assumes the form (5) or (9) of the wave function to hold everywhere, and uses them in computing the exciton energy. This is therefore a purely variational approach, which is affected by the usual shortcomings of variational approaches, namely to give a worse description of wave functions than of energy. This can explain the difference between the bulk P value determined by this approach when $L \to \infty$, and that determined for semi-infinite crystals in Ref. 8.

We have shown that the exciton quantization is mainly determined by the center-of-mass motion for $L > 2.5a_B$, in contrast with previous suggestions of excitons following the electron and hole separation quantization.[13] A simple relation between exciton energy and transition-layer depth $1/P$ holds for $L > 16a_B$. We suggest that absorptance or transmittance experiments in this range, with the further limitation $L \ll \lambda/2$ in order to avoid polaritonic effects, may yield a clear-cut determination of the transition-layer depth.

APPENDIX

In the effective-mass approximation, the Wannier exciton Hamiltonian is

$$H_{\rm ex} = -\frac{\hbar^2}{2M}\frac{d^2}{dZ^2} - \frac{\hbar^2}{2\mu}\Delta_r - \frac{e^2}{\epsilon_0 r} , \tag{A1}$$

where M is the total mass of the exciton, μ the reduced mass, and $\mathbf{r}=\mathbf{r}_e-\mathbf{r}_h$, $Z=(m_e z_e + m_h z_h)/M$. Considering the lowest even and odd exciton wave functions (5) and (9) of the text as trial functions with respect to the variational parameters a and P, we must minimize the quantity

$$\langle \Psi | H_{\rm ex} | \Psi \rangle / \langle \Psi | \Psi \rangle , \tag{A2}$$

where

$$\langle \Psi | H_{\rm ex} | \Psi \rangle = \frac{2}{a^2}\int_0^L [\alpha_1 I_1(z) + \alpha_2 I_2(z) + \alpha_3 I_3(z) + \alpha_4 I_4(z)]\exp(-2z/a)\,dz , \tag{A3}$$

$$\langle \Psi | \Psi \rangle = \frac{2}{a^2}\int_0^L \alpha_0 I_1(z)\exp(-2z/a)\,dz , \tag{A4}$$

$z = z_e - z_h$,

and

$$\alpha_0 = \frac{a}{2} + z, \quad \alpha_1 = \frac{3\hbar^2}{4\mu a} - \frac{e^2}{\epsilon_0} - \frac{\hbar^2}{2\mu a^2} z ,$$
$$\alpha_2 = \frac{\hbar^2}{\mu a} z, \quad \alpha_4 = -\frac{\hbar^2}{2\mu}\left[\frac{a}{2} + z\right] , \tag{A5}$$
$$\alpha_5 = -\frac{\hbar^2}{2M}\left[\frac{a}{2} + z\right] .$$

The integrals $I_1(z)$, $I_2(z)$, $I_3(z)$, $I_4(z)$, and $I_5(z)$ are computed from the even and odd exciton wave functions.

For the even case we get

$$I_1^e(z)=\left[\frac{1}{2K}\sin(KZ)\cos(KZ)+\frac{1}{4P}\sinh(2PZ)\{[F_{eo}(z)]^2+[F_{ee}(z)]^2\}\right.$$
$$+\frac{Z}{2}\{[F_{ee}(z)]^2-[F_{eo}(z)]^2+1\}-\frac{1}{2P}F_{ee}(z)F_{eo}(z)\cosh(2PZ)$$
$$-\frac{2F_{ee}(z)}{K^2+P^2}[P\sinh(PZ)\cos(KZ)+K\cosh(PZ)\sin(KZ)]$$
$$\left.+\frac{2F_{eo}(z)}{K^2+P^2}[P\cosh(PZ)\cos(KZ)+K\sinh(PZ)\sin(KZ)]\right]_{Z_2(z)}^{Z_1(z)}, \tag{A6}$$

$$I_2^e(z)=\left[\frac{F'_{eo}(z)}{P^2+K^2}[P\cosh(PZ)\cos(KZ)+K\sinh(PZ)\sin(KZ)]\right.$$
$$-\frac{F'_{eo}(z)}{P^2+K^2}[P\sinh(PZ)\sin(KZ)+K\cosh(PZ)\sin(KZ)]+\frac{1}{4P}\sinh(2PZ)[F_{ee}(z)F'_{ee}(z)+F_{eo}(z)F'_{eo}(z)]$$
$$\left.-\frac{1}{4P}\cosh(2PZ)[F_{ee}(z)F'_{eo}(z)+F_{eo}(z)F'_{ee}(z)]-\frac{Z}{2}[F_{eo}(z)F'_{eo}(z)-F_{ee}(z)F'_{ee}(z)]\right]_{Z_2(z)}^{Z_1(z)}, \tag{A7}$$

$$I_4^e(z)=\left[-\frac{K}{2}\sin(KZ)\cos(KZ)-F_{ee}(z)\frac{P^2-K^2}{P^2+K^2}[P\sinh(PZ)\cos(KZ)+K\cosh(PZ)\sin(KZ)]\right.$$
$$-F_{eo}(z)\frac{K^2-P^2}{K^2+P^2}[P\cosh(PZ)\cos(KZ)+K\sinh(PZ)\sin(KZ)]$$
$$+\frac{P}{4}\{[F_{ee}(z)]^2+[F_{eo}(z)]^2\}\sinh(2PZ)-\frac{P}{2}F_{ee}(z)F_{eo}(z)\cosh(2PZ)$$
$$\left.-\frac{K^2}{2}Z+\frac{P^2}{2}Z\{[F_{ee}(z)]^2-[F_{eo}(z)]^2\}\right]_{Z_2(z)}^{Z_1(z)}, \tag{A8}$$

where $Z_1(z)=L/2-m_h z/M$, $Z_2(z)=-L/2+m_e z/M$, $F'_{ee}(z)=dF_{ee}(z)/dz$, and $F'_{eo}(z)=dF_{eo}(Z)/dz$. The integral $I_3^e(z)$ has the same analytical form as $I_2^e(z)$, but changing the first derivatives of $F_{ee}(z)$ and $F_{eo}(z)$ by the second derivatives: $F'_{ee}(z)\to F''_{ee}(z)$, $F'_{eo}(z)\to F''_{eo}(z)$.

Analogously, for the odd exciton wave function,

$$I_1^o(z)=\left[-\frac{1}{2K}\sin(KZ)\cos(KZ)+\frac{1}{4P}\sinh(2PZ)\{[F_{oe}(z)]^2+[F_{oo}(z)]^2\}\right.$$
$$+\frac{Z}{2}\{[F_{oo}(z)]^2-[F_{oe}(z)]^2+1\}-\frac{1}{2P}F_{oe}(z)F_{oo}(z)\cosh(2PZ)$$
$$+\frac{2F_{oe}(z)}{K^2+P^2}[P\cosh(PZ)\sin(KZ)-K\sinh(PZ)\cos(KZ)]$$
$$\left.-\frac{2F_{oo}(z)}{K^2+P^2}[P\sinh(PZ)\sin(KZ)-K\cosh(PZ)\cos(KZ)]\right]_{Z_2(z)}^{Z_1(z)}, \tag{A9}$$

$$I_2^0(z)=\left[\frac{F'_{oe}(z)}{P^2+K^2}[P\cosh(PZ)\sin(KZ)-K\sinh(PZ)\cos(KZ)]\right.$$
$$-\frac{F'_{oo}(z)}{P^2+K^2}[P\sinh(PZ)\sin(KZ)-K\cosh(PZ)\cos(KZ)]+\frac{1}{4P}\sinh(2PZ)[F_{oe}(z)F'_{oe}(z)+F_{oo}(z)F'_{oo}(z)]$$
$$\left.-\frac{1}{4P}\cosh(2PZ)[F_{oe}(z)F'_{oo}(z)+F_{oo}(z)F'_{oe}(z)]+\frac{Z}{2}[F_{oo}(z)F'_{oo}(z)-F_{oe}(z)F'_{oe}(z)]\right]_{Z_2(z)}^{Z_1(z)}, \tag{A10}$$

$$I_4^o(z)=\left[\frac{K}{2}\sin(KZ)\cos(KZ)+F_{oe}(z)\frac{P^2-K^2}{P^2+K^2}[P\cosh(PZ)\sin(KZ)-K\sinh(PZ)\cos(KZ)]\right.$$
$$+F_{oo}(z)\frac{K^2-P^2}{K^2+P^2}[P\sinh(PZ)\sin(KZ)-K\cosh(PZ)\cos(KZ)]+\frac{P}{4}\sinh(2PZ)\{[F_{oe}(z)]^2+[F_{oo}(z)]^2\}$$
$$\left.-\frac{P}{2}F_{oe}(z)F_{oo}(z)\cosh(2PZ)-\frac{K^2}{2}Z+\frac{P^2}{2}Z\{[F_{oo}(z)]^2-[F_{oe}(z)]^2\}\right]_{Z_2(z)}^{Z_1(z)}. \tag{A11}$$

The integral $I_3^o(z)$ has the same analytical form as $I_2^o(z)$, but we have to replace the first derivatives of $F_{oo}(z), F_{oe}(z)$ with the second derivatives. The quantities $F_{ee}(z)$, $F_{eo}(z)$, $F_{oe}(z)$, and $F_{oo}(z)$ are given by Eqs. (6), (7), (10), and (11) of the text.

Finally, we have to minimize numerically Eq. (A2) as a function of the parameters a and P. The results are shown in Figs. 1–3.

[1]S. I. Pekar, Zh. Eksp. Teor. Fiz. **33**, 1022 (1957) [Sov. Phys.–JETP **6**, 785 (1958)]; Fiz. Tverd. Tela (Leningrad) **4**, 1301 (1962) [Sov. Phys.–Solid State **4**, 953 (1962)]; *Crystal Optics and Additional Light Waves* (Benjamin/Cummings, London, 1983).

[2]J. Hopfield and D. G. Thomas, Phys. Rev. **132**, 563 (1963).

[3]P. Halevi and G. Hernandez-Cocoletzi, Phys. Rev. Lett. **48**, 1500 (1982).

[4]P. Halevi, in *Excitons in Confined Systems,* Vol. 25 of *Springer Proceedings in Physics,* edited by R. Del Sole, A. D'Andrea, and A. Lapiccirella (Springer-Verlag, Berlin, 1988).

[5]A. D'Andrea and R. Del Sole, Solid State Commun. **19**, 207 (1979).

[6]A. D'Andrea and R. Del Sole, Phys. Rev. B **25**, 3714 (1982).

[7]A. D'Andrea and R. Del Sole, Phys. Rev. B **29**, 4782 (1984).

[8]A. D'Andrea and R. Del Sole, Phys. Rev. B **32**, 2337 (1985).

[9]K. Cho and M. Kawata, J. Phys. Soc. Jpn. **54**, 4431 (1985).

[10]K. Cho, J. Phys. Soc. Jpn. **55**, 4113 (1986).

[11]G. Bastard, E. E. Mendez, L. L. Chang, and L. Esaki, Phys. Rev. B **26**, 1974 (1982).

[12]Y. Shinouza and M. Matsuura, Phys. Rev. B **28**, 4878 (1982).

[13]L. Schulthets, K. Kohler, and C. W. Tu, in Ref. 4, p. 110.

[14]A. D'Andrea and R. Del Sole, Phys. Rev. B **38**, 1197 (1988).

[15]V. A. Kiselev, I. V. Makarenko, B. S. Razbirin, and I. N. Ural'tsev, Fiz. Tverd. Tela (Leningrad) **19**, 2348 (1977) [Sov. Phys.—Solid State **19**, 1374 (1977)].

[16]A. D'Andrea and R. Del Sole, in Ref. 4, p. 102.

[17]K. Cho and H. Ishihara (unpublished).

[18]I. Broser, K.-H. Pantke, and M. Rosenzweig, Solid State Commun. **58**, 441 (1986).